Towards Resistance-free Hydraulics in Construction Machinery

Tekn. Lic. Kim Heybroek

Volvo Construction Equipment, Eskilstuna, Sweden
E-mail: kim.heybroek@volvo.com

Ir. Georges Vael

Innas BV, Breda, Netherlands
E-mail: gvael@innas.com

Professor Jan-Ove Palmberg

Fluid and Mechatronic Systems, Linköping University, Linköping, Sweden
E-Mail: jan-ove.palmberg@liu.se

Abstract

The topic of resistance-free motion control refers to solutions that minimize or completely eliminate the need for proportional valves, hence avoiding the throttling losses associated with metering. Previous research by the authors shows how a secondary control system could be used to improve energy efficiency in construction machines. The proposed solution uses hydraulic transformers, powered by a common pressure rail system driving both the linear work implements and the rotary drives of a propulsion system in a wheel loader.

An emphasis in this paper is on the sizing aspects of transformer-based system design. The solution under special observation enables the use of smaller transformers utilizing the differential cylinder as a two-stage gearbox by means of “short-circuiting” its two cylinder chambers.

The results and outlook from this study touch on how state-of-the-art secondary control systems could improve the energy efficiency of future construction machinery and suggest potential areas of improvement.

KEYWORDS: hydraulic transformer, secondary control, wheel loader, CPR, sizing

1. Resistance-free power transformation

In the quest to find the most energy efficient motion control system for construction machines, so called secondary control systems (SCS) are sometimes suggested as a promising solution. Secondary control as a research topic has its origins in the early 80s /1/, /2/. However, also in much more recent publications this technology has demonstrated promising results in both theory and practice /3–5/.

However, applying this technology to construction machines, there is clearly also a need for solutions to how linear-mechanic actuators should be controlled without excessive throttling losses as a result.

As is well known, the force produced by a hydraulic cylinder is the product of cylinder area and the pressure. If continuously variable force control in an SCS is required, no solution exists where the cylinder area is the controlled variable. However, recent studies /6/ show how switching control of 'multi-chamber cylinders' can be used to realize force control by means of a discretely variable cylinder area. The second alternative is to modulate the cylinder pressure. Valve control could be used to adapt the given, quasi-static SCS pressure level to the load pressure but this would lead to excessive power losses. A 'resistance-free' solution is needed, which can transform the SCS pressure level to the load pressure level without any principle losses. **Figure 1** compares the principle of transformation to that of throttling.

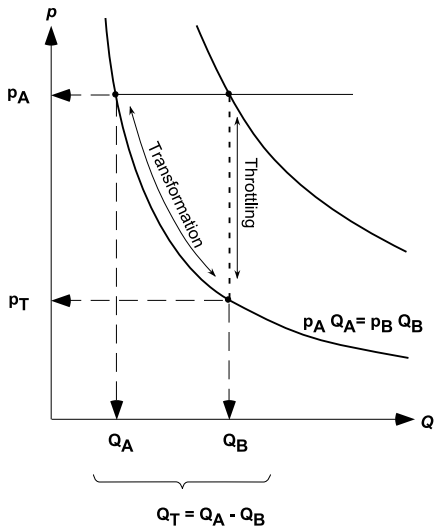

Figure 1: The principle of hydraulic transformation versus throttle control

The figure shows that any type of hydraulic transformer needs a ratio between its input and its output flow. The pressure transformation ratio is inversely proportional to this flow ratio.

In the early days of secondary control studies, a rotary hydraulic transformer type was conceived, that realizes the required flow ratio by simply coupling two axial piston hydrostatic units /7/, /8/. As the units rotate at the same speed, the flow ratio is equal to the displacement ratio. By having one or both units variable, the flow ratio - and with that the pressure transformation ratio - could be made continuously variable.

Due to its bulkiness, its rather poor efficiencies and its high cost, this hydraulic transformer concept never found applications beyond some niche markets.

The Innas Hydraulic Transformer (IHT) concept aims to solve the weak points of that old axial piston transformer design. In the original IHT design /9/ shown in the left part of **Figure 2**, a variable flow ratio is realized by exchanging the two-kidney port plate of a standard axial piston pump or motor, for a port plate with three ports, which typically span 120 degrees each. One port is connected to the supply circuit, another to the load circuit and the third to the make-up circuit. The port-plate can be rotated over a limited angle. This changes the angular position of each port with respect to the point where the pistons reach Top Dead Centre. Each port thus defines a window for the sine-shaped movement of the pistons. Consequently, a different part of the piston flow will enter or leave the machine through each port. In this way, the port-plate control angle ∂ determines the flow ratio between supply and load port and a continuously variable hydraulic transformer is realized. The variation of the relative angle ∂ can be realized by turning the port-plate but also by turning the element that determines the movement of the pistons. This latter solution was used in a more recent IHT design for automotive use /10/, shown to the right in Figure 2. In /11/, an IHT design is presented, in which the relative angle ∂ is realized in a yet another way.

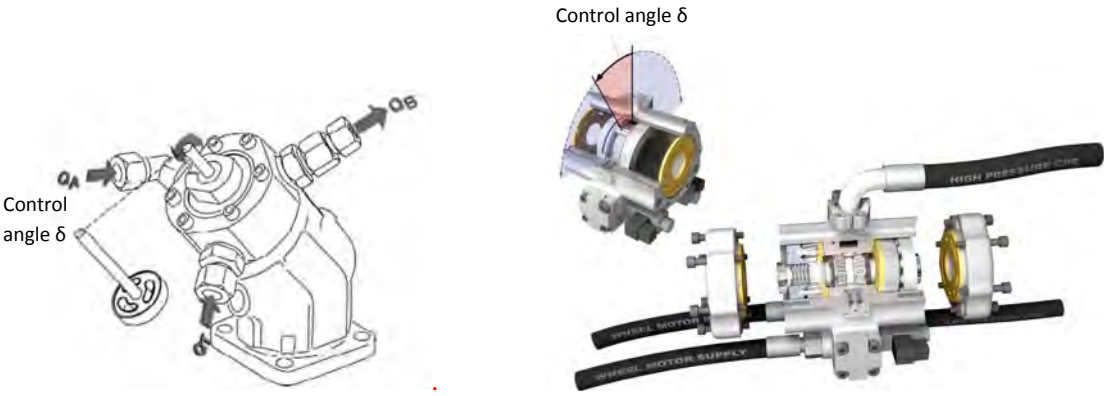

Figure 2: (Left) IHT –bent axis design. (Right) IHT - recent floating cup design.

The equation for the transformation ratio of a lossless IHT with three kidneys, each 120 degrees long, is:

$$\Pi = \frac{p_B}{p_A} = \frac{-sin(\delta) - \frac{p_T}{P_A} sin\left(\delta + \frac{2\pi}{3}\right)}{sin\left(\delta - \frac{2\pi}{3}\right)} \quad (1)$$

The equation for the flow, also neglecting losses, of the load port of this design is:

$$Q_B = -\frac{\omega}{2\pi} \cdot V_{IHT} \cdot sin\left(\delta - \frac{2\pi}{3}\right) \cdot sin\left(\frac{\pi}{3}\right) \quad (2)$$

A detailed derivation of these equations is outside the scope of this article but can be found for instance in /9/, /12/ and /13/. With the equations, curves can be plotted for ∏ and for $2\pi \cdot Q_B/(\omega \cdot V_{IHT})$ as a function of ∂. These curves are shown in **Figure 3**.

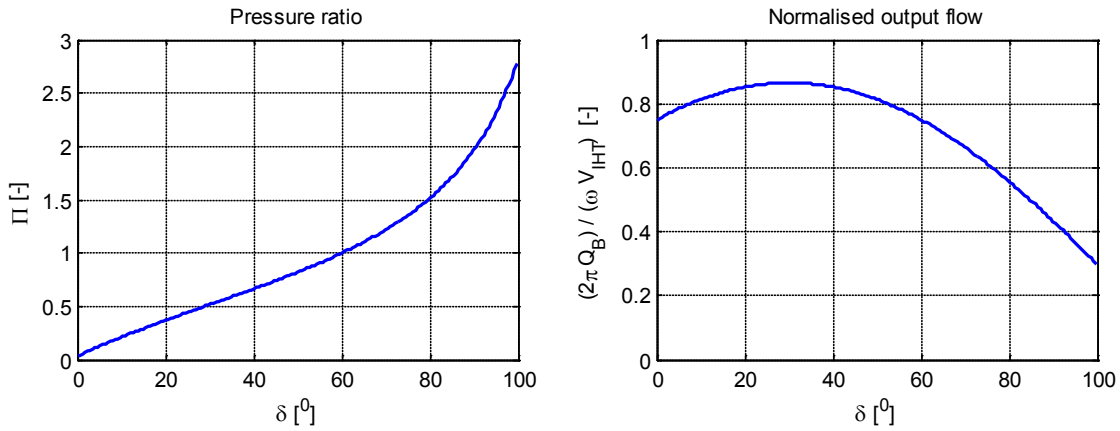

Figure 3: Transformation curves

The magnitude of the control angle of the IHT essentially sets the output pressure level; the sign of the control angle determines at which of the IHT ports this pressure is realized. If the sign goes from positive to negative, the output port and the make-up port switch function. The reaction of the load to the IHT's output pressure determines whether the IHT is providing or recuperating energy.

2. The wheel loader application

In this paper a wheel loader is used as an example to illustrate how construction machinery may benefit from a transformer-based secondary control system. The wheel loader studied here is a Volvo L220, which uses a drop-box type mechanical transmission for the wheel drive, with 4 forward and 4 reverse gears, a lockable hydrodynamic torque converter between the engine and the gear transmission, and fully floating axle shafts with planetary-type hub reductions. The hydraulic system has

two load-sensing axial piston pumps and an extra pump for the fan drive and brake accumulator charging. The double-acting hydraulic work cylinders for the lift and tilt functions are controlled by means of double-acting closed centre spool valves.

The pie chart in **Figure 4** shows an estimate of the machine usage over an average working day for a large-end Volvo wheel loader. As shown in the figure, the short cycle loading (SCL), sometimes referred to as the Y-cycle, is the most common duty cycle and is therefore used as a reference in this paper.

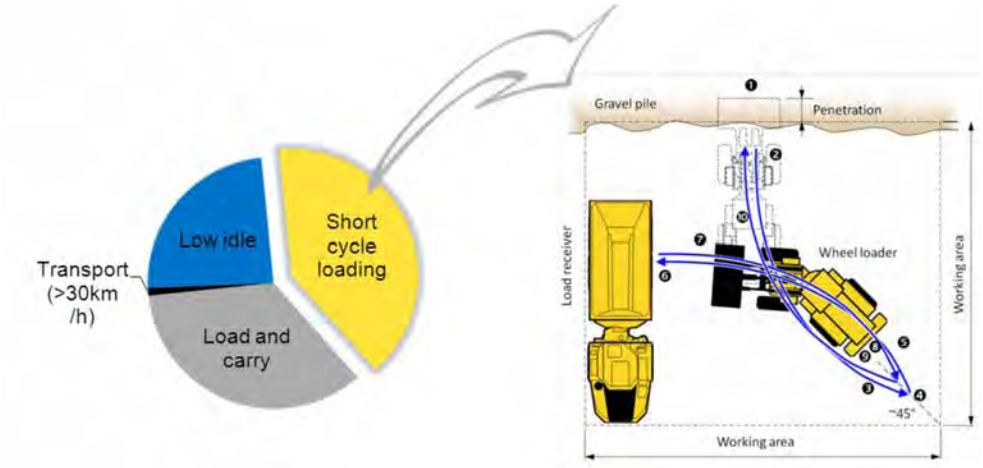

Figure 4: Distribution in customer machine usage and illustration of the short cycle loading. The figure to the right is reprinted by kind permission of /19/

3. System proposal

In theoretical studies, the IHT solution has been applied to various construction machines /15–17/. In a previous study by the authors, an IHT-based secondary control system was proposed for the wheel loader /18/, with the schematics shown in **Figure 5**. For the Y-cycle (operated at high pace), a 50% reduction in fuel consumption was shown through simulation. The main reasons for the fuel saving are the decoupling of individual actuators and decoupling of the engine, eliminating the problem with losses in parallel operation and enabling improved engine management strategies. Moreover, the system allows for energy recuperation in both work hydraulics and propulsion. In the new transmission, a transfer case with two identical constant displacement motors replaces the old mechanical transmission and the torque converter. One of the two motors has an extra gear transmission while the other is directly connected to the transfer case. The motors work in all 4 quadrants, which means they can double as a pump while braking, regenerating energy back to the CPR. The motors are driven individually or together by means of a single hydraulic transformer. For controlling and driving the hydraulic cylinders, three additional hydraulic transformers are connected to

the CPR. For the lift and tilt functions, four logical valves arranged in an H-bridge configuration enable an energy efficient 4-quadrant control in two different modes of operation, discussed in greater detail in the following section.

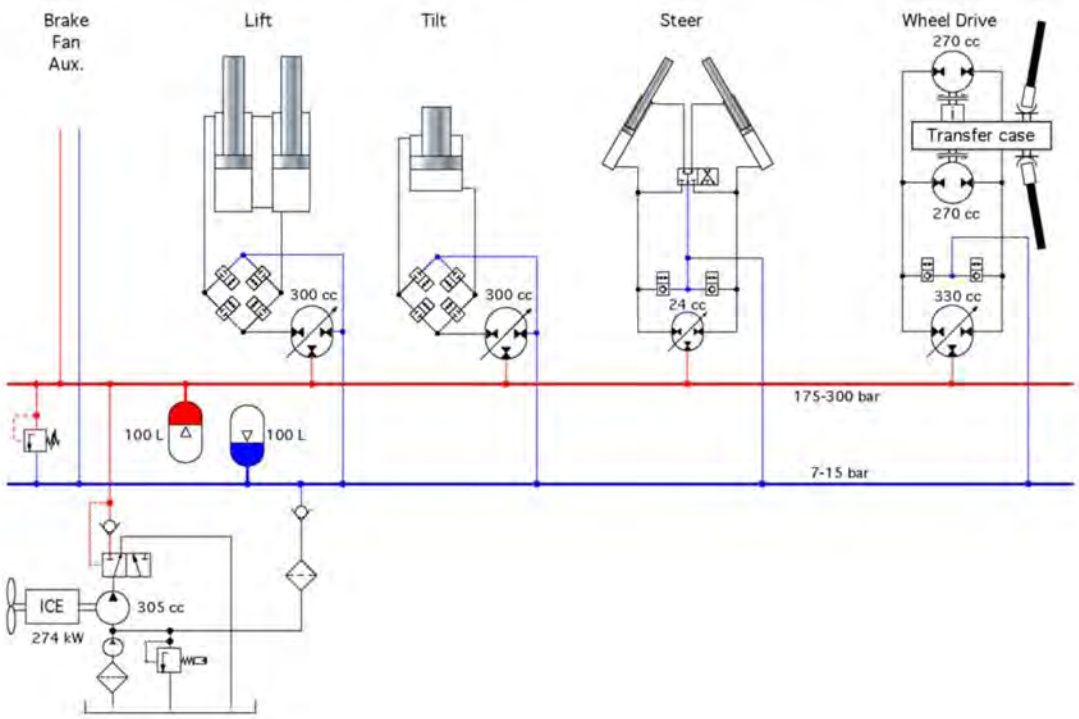

Figure 5: The proposed hydraulic circuit based on a common pressure rail with hydraulic energy storage in accumulators and hydraulic transformers

3.1. The work hydraulics

Since the new drive system requires one hydraulic transformer per actuator, it is very important to use as small components as possible to minimize the penalty in cost. **Figure 6** shows the current maximum theoretical working range for the lift function in force and speed. In the passive quadrants (Q1 and Q3), the working range is determined by cylinder piston area along with the maximum pump flow and its maximum working pressure. In the overrunning quadrants (Q2 and Q4), the maximum speed is more than twice as high, achieved by means of meter-out valve control. The figure also shows two measured force and speed traces for two Y-cycles, differing both in pace and loaded material. In these cycles, both the lift and the tilt function display a moderate maximum speed in the passive quadrants and a very high maximum speed in only the second (overrunning) quadrant, while Q3 and Q4 are hardly used at all. Of course, this might look very different in other cycles. The figure also shows, in grey shading, the regions of the current operating range that are rarely used and could therefore be considered over-spec. The IHT's size is mainly determined by the

maximum power that it has to deliver /9/. Hence, the current maximum operating range has to be translated into a maximum power requirement. For the lift function, this is shown in the right part in Figure 6.

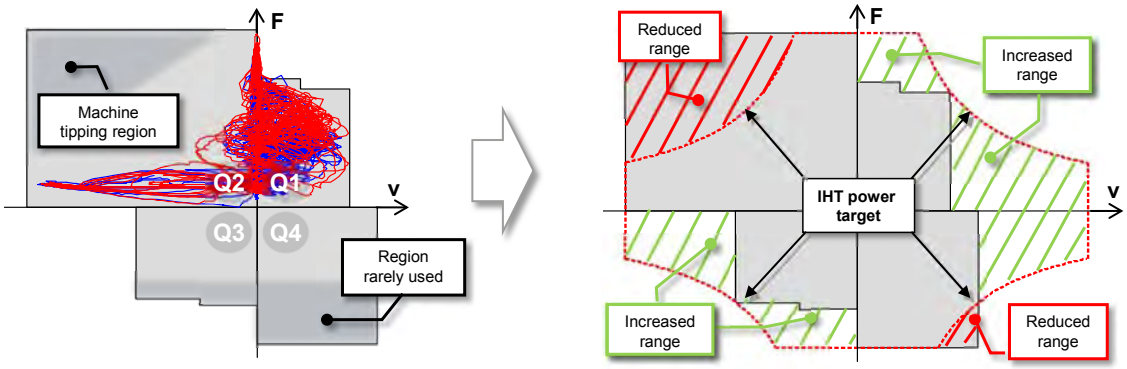

Figure 6: (Left) Schematic illustration of working range and its limitations given normal customer usage and other system limitations. (Right) The consequent targeted IHT power level and resulting trade-offs in operating region

Different valve arrangements may be used to control a differential cylinder with a hydraulic transformer /13/. In the proposed hybrid system, an H-bridge valve arrangement is adopted for both the lift and the tilt function, as shown in **Figure 7**. With this arrangement, the differential cylinder can be operated as a two-stage gearbox by means of short-circuiting its two cylinder chambers /19/. In this way, two modes of operation for the IHT are created, which allows for a greater theoretical operating range for a given IHT size. As shown in Figure 6 this is especially important in the second quadrant. As a result, smaller IHTs can be chosen which will operate closer to their efficiency sweet-spot. The proposed circuit in Figure 7 also shows an optional fifth valve between the two cylinder chambers, which can simplify mode switching /20/.

In order to visualize and check the ability of a certain IHT size to cover the required region of operation, equations (1) and (2) are used. For known levels of p_A and p_T, equation (1) gives the load pressure p_B as a function of the control angle ∂. For a certain V_{IHT} and its maximium speed, equation (2) yields the IHT's maximum flow as a function of ∂. With the cylinder area that the IHT acts on, these equations translate to equations for the cylinder force F and the cylinder speed v as a function of ∂. Plotting F and v for each ∂, results in a typical nose-shaped curve, which represents the ideal range limits for the chosen V_{IHT}, its n_{max} and rail pressures p_A and p_T. Also taking into account the losses of all components, this curve has to match the required maximum power curve. The characteristic 2-stage IHT range is visualized to the right in Figure 7.

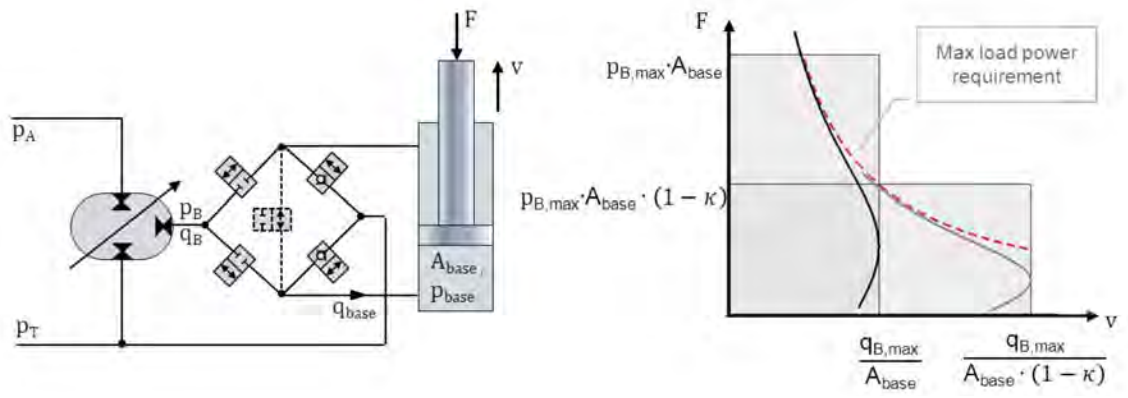

Figure 7: (Left) Transformer, valve and cylinder arrangement enabling 4-quadrant operation and multi-mode operation. (Right) Illustration of how the IHT flow and pressure translate to load force and speed given the two modes of operation.

For both the lift and the tilt function, the sizing of the cylinder areas and the IHT follows the same steps:

First, from the known 1st quadrant maximum force for the current system and a chosen maximum cylinder pressure, the minimum base side area for the cylinder can be determined as:

$$A_{base,min} = \frac{F_{Q1,max}}{p_{cyl,max} - \kappa \cdot p_T} \tag{3}$$

In this equation, κ is the ratio between the ring area and the base area. This ratio eventually determines the ratio between the two 'gear-steps' of the cylinder (see also Figure 7) and is still unknown at the start of the sizing process. To stay on the safe side, a maximum value for κ of 0.75 is assumed (which corresponds to a ratio of 4 between the gear steps). The maximum pressure in both lift and tilt cylinder is 36 MPa. Through its amplification capability, the IHT can always realize this value, even if the supply pressure is at the lower accumulator pressure boundary (set here to 20 MPa).

Then, in a similar manner, the minimum ring side area for the cylinder can be determined from the known 3rd quadrant maximum force for the current system and the same chosen maximum cylinder pressure:

$$A_{ring,min} = \frac{|F_{Q3}|_{,max}}{p_{cyl,max} - \frac{p_T}{\kappa}} \tag{4}$$

In this case, 0.5 is used as the worst case minimum value of κ (a ratio of 2 between gear steps).

Assuming that – in order to avoid buckling - the cylinder rod size may not be smaller than it is in the current system, a third boundary for A_{ring} and A_{base} can be determined:

$$A_{ring} \leq A_{base} - A_{rod,current} \quad (5)$$

The three boundaries together define a field of possible combinations of A_{base} and A_{ring}. Next, an appropriate IHT size has to be chosen; this is done by combining equations (1) and (2) into a relationship for the IHT's maximum power as a function of p_A and p_T:

$$P_B = Q_B \cdot (p_B - p_T) = \frac{\omega_{max}}{2\pi} \cdot V_{IHT} \cdot sin\frac{\pi}{3} \cdot (p_A - p_T) \cdot \sin(\delta) \quad (6)$$

As has been shown in Figure 6, the required maximum power is defined by the corner power point in the first quadrant. This requirement also has to be met when the CPR pressure difference (p_A –p_T) is at its minimum value. In that case, the control angle ∂ is close to its maximum of 100º. With this, equation (6) yields the minimal required V_{IHT}: 240 cm^3 for both the lift and the tilt function

With this V_{IHT} and its calculated energy loss map, a load cycle simulation was performed for a number of combinations of A_{base} and A_{ring}. For each function, the simulations calculate the energy that flows into its IHT during the SCL. The switchover strategy between the two cylinder 'modes' consisted of using the 'low force / high speed' mode as much as possible. Only if the required forces are too large, the 'high force / low speed' mode is used. p_A was set to to 20 MPa (worst-case), p_T to 1 MPa.

This calculation was done for both the lift and the tilt function. The resulting contour plots for the total net energy that each transformer draws from the CPR during the SCL are shown in **Figure 8**. In order to arrive at a relative number, the net energy drawn from the rail was divided by the total energy that enters the cylinder in the passive quadrants of the same SCL.

The figure shows that a lift cylinder with a base area of 460 cm^2 and a ring area of 340 cm^2 would be optimal from an energy point of view. For this optimal combination of component sizes, all points of operation of the Y-cycle can be covered. Nevertheless, a large region of the 2nd quadrant cannot be reached. Therefore, the base area has been increased to 500 cm^2 while keeping the ring area at 340 cm^2. As can be seen in the contour plot for the lift function in Figure 8, this has a minor effect on energy efficiency. The effect of the IHT on the energy efficiency was also studied. It turned out that the IHT size could be increased to 300 cm^3, with the advantage of an equivalent increase in operation range, without decreasing the overall efficiency.

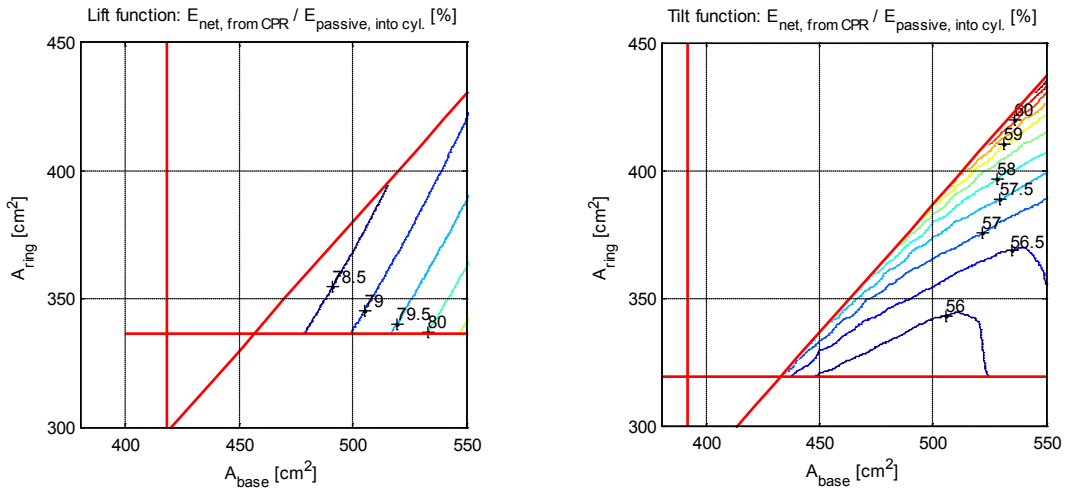

Figure 8: Net energy taken by the IHT from the CPR divided by the net energy required by the load in the passive 1st and 3rd quadrants. (Left): Lift function, (Right): Tilt function

The simulation result for this set of parameters is summarized in a so-called 'bubble-plot', shown in Figure 9. The area of each bubble is a measure of the amount of energy that the cylinder drive requires from or gives back to the rail at the point of operation indicated by the centre of the bubble. The blue and red areas represent the operating points that the IHT-driven cylinder can reach in normal (blue) or short-circuited mode (red). The limits of the operation region are calculated taking to the efficiency of the transformer, estimated from measurements, into account. In the background of the figure, the light grey areas show the possible operation region of the current system.

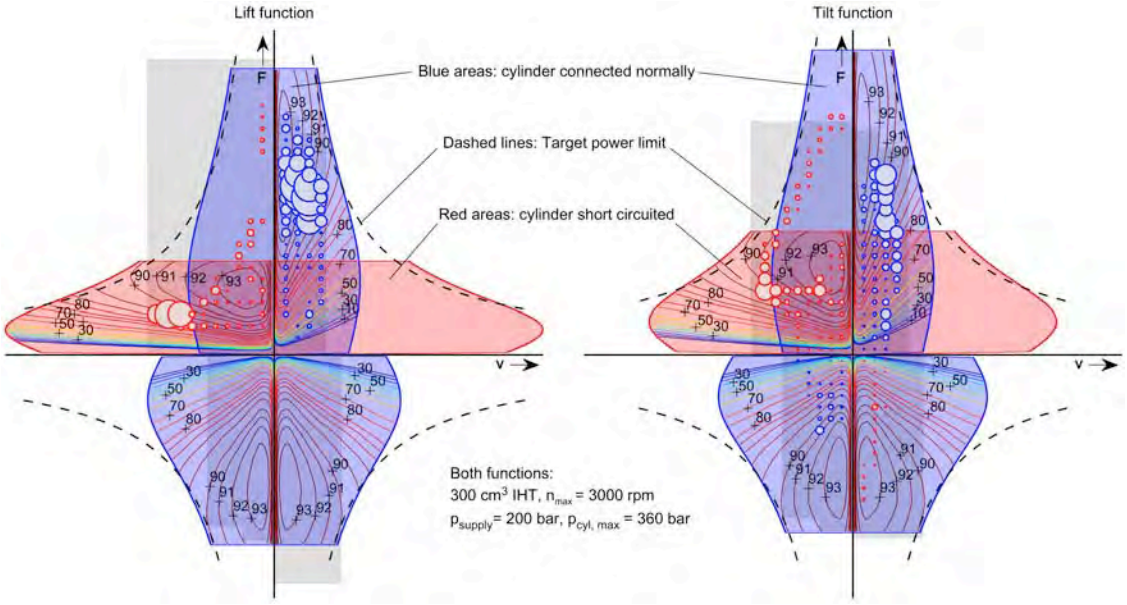

Figure 9: Optimization result for the lift (left) and tilt (right) function

With these parameters, the SCS system outperforms the current system by far in the 1st, the 3rd and the 4th quadrant, allowing for quicker operation. In the 2nd quadrant, the current system can reach higher speeds at higher load forces than the SCS system. However, as illustrated with the grey areas in Figure 6, it is debatable whether this is a firm requirement or not. If the meter-out valve of the H-bridge solution is made proportional, it is of course no problem to reach also outside of the IHT working limits in the 2nd quadrant, but it would be by means of throttle-based control /19/. Alternatively the power requirement of the second quadrant could be taken as another boundary condition in the optimization, hence forcing the IHT to cover also this area.

In a similar approach, a good option for the tilt function was determined to be an A_{base} of approx. 530 cm^2 and an A_{ring} of approx. 320 cm^2, combined with an FCT size of again 300 cm^3. The simulation results for this function are also shown in **Figure 9**.

The steer function was also sized and simulated. For space reasons and because it represents a far lower energy consumption, it is not treated in this paper.

3.2. The propulsion system

As mentioned earlier, the new wheel drive system consists of one IHT and two identical constant displacement units. One of these units is connected directly to the transfer case, the other through an extra gear transmission. By coupling either one or both units to the transfer case, three discrete gear steps are realized. **Figure 10** aims to illustrate the range of the new drive system relative to that of the baseline system.

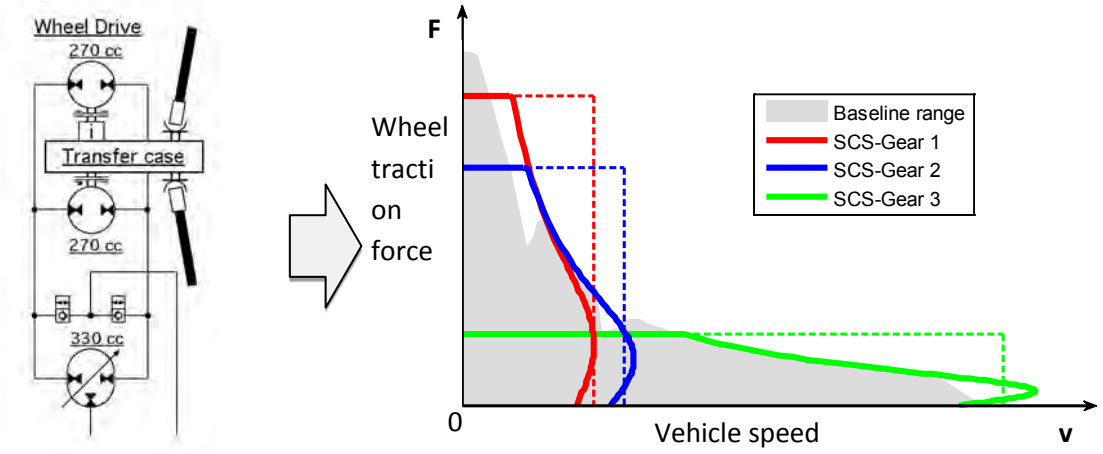

Figure 10: Schematic of the 3-gear IHT wheel drive and how it sufficiently compares to the range of the baseline system

The limitations for each gear have their own colour. The solid lines represent the limitations imposed by the transformers, while the dashed lines are the limitations

imposed by the hydraulic motors. The curves were calculated using the same equations as for the work hydraulics, including the relevant component losses estimated from measurements.

The sizing the wheel drive system was not primarily focused on efficiency optimality, but rather on finding a good coverage of the required region of operation.

The starting point for this sizing process is the required maximum wheel force. Through its amplification capability, the IHT can always realize a 50 MPa maximum pressure difference over the hydraulic motors. Together with the maximum wheel traction requirement and the transmission ratio between transfer case and wheels, including losses of all components, this translates to a minimum total displacement of the motors of 1150 cm^3. Here again, the size of the IHT is determined based on a maximum load power requirement. The size of the directly coupled drive unit is maximized by the maximum speed requirement and the IHT size. Taking all these restrictions into account, the resulting drive system consists of: two 270 cm^3 drive motors, one directly coupled and one through a gear ratio of 3.3, and a 329 cm^3 IHT.

Figure 11 shows the effect of this solution. The targeted load power requirement is indicated by the dashed line. The figure shows that with the selected component sizes, the area underneath this dashed line is adequately covered.

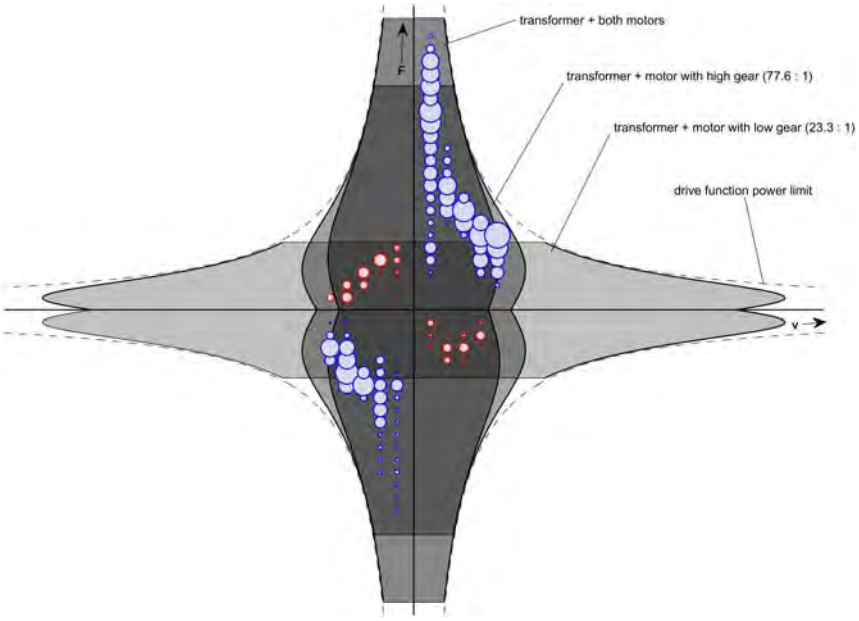

Figure 11: Sizing of the 2-motor and transformer combination for propulsion

The figure also shows the result of a simulation of a representative Y-cycle. Again, the area of each bubble represents the amount of energy that the wheel drive requires or gives back to the rail in the point of operation indicated by the centre of the bubble.

3.3. Limitations and method considerations

The drawback of the suggested approach is that the resulting component sizes are only optimal under the condition that the new system is operated in exactly the same way as the reference system. Since the suggested system has very different characteristics and operating range compared to the old system, the suggested approach is only relevant if the operator is actively prevented from working outside the limits of the old system. However, as Zhang et al. correctly noted /21/: “The job is task-oriented, not reference-oriented”. The task in this case is to achieve some level of productivity (ton/h) at as low fuel consumption (l/h) as possible. So, if the new drive system would allow higher productivity, also desired by the operator, the optimization should ideally also include the effect of changed operator behaviour. However, this requires sophisticated operator models or human in the loop simulators working with detailed environment models /14/, /22/. Since greater productivity generally requires larger components the cost aspect must also be taken into account. This could be done through a total cost of ownership (TCO) calculation, weighing the benefits of fuel efficiency benefits against their cost. None of these aspects were implemented in the evaluation and sizing of the proposed system, but are definitely interesting topics for future studies.

4. Results and Future Work

In this study the conventional drive system of a large wheel loader was replaced with a secondary control system. The new system uses hydraulic accumulators for energy storage and one rotary hydro-mechanical transformer of IHT type per actuator. Simulation shows that the new system may reduce fuel consumption by up to 50% in selected duty cycles (Y-cycle).

The transformers driving both the work hydraulics and each individual work hydraulic function were optimized with respect to maximum efficiency and minimum size. 4-quadrant operation of cylinder drives is achieved by means of a valve arrangement using four or five individual valves. A differential mode of operation allows both smaller transformers and higher cycle efficiency. For the propulsion system, the required range of operation is achieved by two equally sized hydraulic motors with different mechanical gear ratios being driven by one transformer. **Table 1** shows the high level

result from the complete sizing process side by side with the predicted system efficiency gains, presented earlier in /18/. Important to note is that the performance improvements presented here are based on simulations of the Y-cycle only. Further analysis is required determine out how well the system meets the requirements of other duty cycles. The proposed solution is a full-fledged SCS-IHT solution, but for future studies, also 'mild' versions of the technology could be of interest.

	Components / subsystems	Volvo L220-Baseline	Volvo L220-SCS
Major hardware changes	Converter+4 gear dropbox	Yes	No
	Installed hydraulic displacement	100%	739%
	Energy storage	No	2 x 100 l. hyd acc.
	Hydraulic cylinders	$A_{base,tot}$:100%, $A_{rod,tot}$:100%	$A_{base,tot}$:94%, $A_{rod,tot}$:154%
Performance improvements	Average engine power	100%	52%
	Losses in hydraulic circuit	100%	22%
	Losses in propulsion system	100%	46%
	Fuel consumption	100%	49%

Table 1: High level summary from the simulation study and the sizing process

There are still many open questions concerning the supply side of the SCS system. For instance, how the system would be impacted if variable displacement pump is used and how such a solution should be controlled for optimum energy efficiency. Also interesting for future studies is to introduce additional gear steps for the linear drives, using parallel cylinders with unequal area ratios. If the resulting number of gear steps is high enough it could even be interesting to consider a purely digital hydraulic cylinder drive, potentially eliminating the need for hydraulic transformers. Open questions in such a direction are for instance, whether adequate controllability can be achieved and what cost penalty could be expected relative to the IHT solution.

5. Nomenclature

Quantities

δ	[rad]	IHT control angle	B_V	[Nms]	viscous friction coefficient
P	[W]	power	V	[cm^3]	machine displacement
p	[bar]	hydraulic pressure	T	[Nm]	torque
Q	[l/min]	hydraulic flow	J	[kgm^2]	inertia
Π	[-]	pressure amplification factor	ω	[rad/s]	rotational velocity
κ	[-]	cylinder area ratio	t	[s]	time

Indices

A	supply side of IHT (connected to CPR)	ring	annular of hydraulic cylinder
B	load side of IHT (connected to load)	base	piston of hydraulic cylinder
T	tank side IHT (connected to CPR)	rod	rod of hydraulic cylinder
Q	load quadrant (1 through 4)		

Abbreviations

CPR	Common Pressure Rail	SCL	Short Cycle Loading
OEM	Original Equipment Manufacturer	ICE	Internal Combustion Engine
IHT	Innas Hydraulic Transformer	ekv	equivalent
SOC	State Of Charge	cyl	cylinder

References

[1] M.-C. Shih, “Untersuchung Einer Zylinderansteuerung durch Hydro-Transformator am Konstant Drucknetz,” Aachen University, Aachen, 1984.

[2] G. Palmgren and J.-O. Palmberg, “Secondary Controlled Hydraulic Systems – A New Drive Concept with Future Prospects,” in *International Fluid Power Exposition, IFPE’88*, 1988.

[3] L. Hartter, A. Birckett, T. Casciani, M. Pomerleau, and M. Subramaniam, “Series Hydraulic Hybrid System for Urban Vehicles,” in *7th International Fluid Power Conference*, 2010.

[4] P. A. J. Achten, “A serial hydraulic hybrid drive train for off-road vehicles,” *NCFP*, vol. 19, no. 2, pp. 515-521, 2008.

[5] S.-an Liu, Y.-min Yao, T. Shang, Y. L. Chen, and M. Miao, “Full hydraulic drive system of minitype loader based on secondary regulation technique,” *Journal of Jilin University*, vol. 41, no. 3, pp. 665-669, 2011.

[6] M. Linjama, H.-P. Vihtanen, A. Sipola, and M. Vilenius, “Secondary Controlled Multi-Chamber Hydraulic Cylinder,” in *The 11th Scandinavian International Conference on Fluid Power, SICFP’09, June 2-4, 2009, Linköping, Sweden*, 2009, vol. 1.

[7] R. Kordak, “Hydrostatische Antriebe mit Sekundärreglerung,” in *Der Hydraulik Trainer, Band 6*, Mannesmann Rexroth, 1989.

[8] K. Dluzik, “Entwicklung und Untersuchung energiesparender Schaltungskonzepte für Zylinderantriebe am Drucknetz,” RWTH Aachen, 1989.

[9] P. A. J. Achten, Z. Fu, and G. E. M. Vael, “Transforming Future Hydraulics: a New Design of a Hydraulic Transformer,” in *Proceedings of the Fifth SICFP Linköping University*, 1997.

[10] P. A. J. Achten, T. L. Van den Brink, J. W. Potma, M. P. A. Schellekens, and G. E. M. Vael, “A four-quadrant hydraulic transformer for hybrid vehicles,” 2009.

[11] P. A. J. Achten and T. L. Van den Brink, “A Hydraulic Transformer with a Swash Block Control Around Three Axis of Rotation,” in *8th International Fluid Power Conference*, 2012.

[12] G. E. M. Vael, P. A. J. Achten, and Z. Fu, “The Innas Hydraulic Transformer - The Key to the Hydrostatic Common Pressure Rail,” *SAE International Off-Highway and Powerplant Congress and Exhibition*, no. 2000-01-2561, 2000.

[13] G. E. M. Vael, P. A. J. Achten, and J. W. Potma, “Cylinder Control with the Floating Cup Hydraulic Transformer,” in *The Eighth Scandinavian International Conference on Fluid Power*, 2003.

[14] R. Filla, A. Ericsson, and J.-O. Palmberg, “Dynamic Simulation of Construction Machinery: Towards an Operator Model,” *IFPE 2005 Technical Conference*, pp. 429-438, 2005.

[15] G. E. M. Vael, E. Orlando, and R. Stukenbrock, “Toward Maximum Flexibility in Working Machinery , IHT Control in a Mecalac Excavator,” no. Dc. 2004.

[16] M. Inderelst, S. Losse, S. Sgro, and H. Murrenhoff, “Energy Efficient System Layout for Work Hydraulics of Excavators,” in *The Twelfth Scandinavian International Conference on Fluid Power, May 18-20, 2011, Tampere, Finland*, 2011.

[17] Y.-min Yao, S.-an Liu, T. Shang, Y. L. Chen, and Z. Xu-hui, “Energy-saving technique for loader ZL50 based on constant pressure hydraulic system,” *Journal of Jilin University*, vol. 41, no. 1, pp. 117-121, 2011.

[18] P. A. J. Achten, G. E. M. Vael, and K. Heybroek, “Efficient hydraulic pumps , motors and transformers for hydraulic hybrid systems in mobile machinery,” in *Wissensforum VDI*, 2011.

[19] K. Heybroek, J. Larsson, and J. O. Palmberg, “Mode Switching and Energy Recuperation in Open-Circuit Pump Control,” in *The Tenth Scandinavian International Conference on Fluid Power, SICFP’07*, 2007.

[20] B. Yao, “Energy-Saving Control of Single-Rod Hydraulic Cylinders with Programmable Valves and Improved Working Mode Selection,” *Proceedings of the 49th National Conference on Fluid Power*, pp. 81-91, 2002.

[21] R. Zhang, D. E. Carter, and A. G. Alleyne, “Multivariable Control of an Earthmoving Vehicle Powertrain Experimentally Validated in an Emulated Working Cycle,” in *ASME International Mechanical Engineering Congress and Exposition, IMECE’03*, 2003, no. 586.

[22] T. S. von Baumgarten, H.-H. Harms, and T. Lang, “Benchmarking Mobile Machines Considering Operator Planning and Control Behaviour,” in *The 12th Scandinavian International Conference on Fluid Power, May 18-20, 2011, Tampere, Finland*, 2011.